PROCEEDINGS OF SCIENCE

The long-distance behaviour of the vector-vector correlator from $\pi\pi$ scattering

Srijit Paul,[a,*] **Andrew D. Hanlon,**[b] **Ben Hörz,**[c] **Daniel Mohler,**[d] **Colin Morningstar**[e] **and Hartmut Wittig**[a,f]

[a] *Institut für Kernphysik, Johannes Gutenberg-Universität Mainz, Johann-Joachim-Becher-Weg 45, D 55128 Mainz, Germany*

[b] *Physics Department, Brookhaven National Laboratory, Upton, New York 11973, USA*

[c] *Nuclear Science Division, Lawrence Berkeley National Laboratory, Berkeley, CA, USA 94720*

[d] *Helmholtzzentrum für Schwerionenforschung (GSI), Planckstrasse 1, 64291 Darmstadt, Germany*

[e] *Department of Physics, Carnegie Mellon University, Pittsburgh, PA 15213, USA*

[f] *PRISMA$^+$ Cluster of Excellence, Johannes Gutenberg-Universität Mainz, Staudingerweg 9, 55128 Mainz, Germany,*

E-mail: spaul@uni-mainz.de

We present the estimation of the long distance behaviour of the vector-vector correlator computed on a lattice QCD ensemble generated with $2+1$ flavour physical Wilson clover quarks. The long distance regime of the correlator is dominated by multi-hadronic scattering states. We reconstruct the correlator in this regime using the $\pi\pi$ scattering states in the $I = 1$ channel. The vector-vector correlator appears in the integrand to estimate the hadronic vacuum polarization contributions to the anomalous magnetic moment of the muon. Therefore, an improved estimation of the correlator will help resolve the tension between $(g-2)_\mu$ experiment and theory.

The 39th International Symposium on Lattice Field Theory, LATTICE 2022
8th-13th August, 2022 Bonn,
Germany

*Speaker

PoS(LATTICE2022)073

1. Introduction

Recently, advances in novel algorithms and improved computational resources have enabled the lattice community to perform simulations using physical quark masses. This marks a significant development because previous simulations used quark masses that were much heavier than those found in nature, making it difficult to accurately model physical phenomena. With the ability to perform simulations using physical quark masses, the lattice community can now access relevant scattering thresholds, which are essential for studying meson-meson, meson-baryon and baryon-baryon scattering systems. This is the reason we often encounter the contributions from the relevant multi-hadronic states in all hadronic observables in our lattice calculations. In this conference there have been several talks depicting the effect of multi-hadronic states such as Nπ contamination in the nucleon structure observables [1, 2].

In this talk, we demonstrate the reconstruction of one such observable relevant for the high precision determination of the hadronic contribution to the anomalous magnetic moment of the muon ($a_\mu^{\rm HVP}$) for flavour f, using the multi-hadronic $\pi\,\pi$ scattering states, which is defined by,

$$\left(a_\mu^{\rm hvp}\right)^f = \left(\frac{\alpha}{\pi}\right)^2 \int_0^\infty dx_0 \frac{G\,(x_0)\,\widetilde{K}\,(x_0)}{m_\mu} \tag{1}$$

where α is the fine structure constant, $\tilde{K}$ is the analytically determined QED kernel and m_μ is the mass of the muon. Due to the small mass of the muon ($\approx$ 105 MeV), the contribution to its anomalous magnetic moment is dominated by low Q^2 values or, in other words, long-distance contributions on hadronic scales. The observable in spotlight receives major non-perturbative long distance contributions from the correlation function of the electromagnetic current of the light quarks, otherwise called the vector-current correlator ($G\,(x_0)$). The $G\,(x_0)$ is an important quantity which relates how individual quarks interact with the electromagnetic current weighted by their corresponding charges. Here, we focus on the light quark(u and d) contributions. The quantum numbers and the low energy regime for the vector correlator helps determine the relevant multi-hadronic states which contribute towards its finite-volume reconstruction.

2. Methodology

Lattice Setup: We performed our measurements on ensembles which were generated using non-perturbatively $O(a)$ improved Wilson fermion action and a tree-level $O(a^2)$ improved Lüscher-Weisz gauge action [3]. The details of the ensemble are given below:

Ensemble Name	Box Size	lattice spacing	$m_\pi L$	$N_{configs}$	Smearing
E250($96^3 \times 192$)	6.2 fm	0.06426 fm	4.1	353	($\rho_{\rm stout}$, $N_{\rm stout}$) = (0.1, 36)

Table 1: Lattice Description

Distillation Setup: We employ the stochastic LapH method to treat all-to-all quark propagators [4, 5] which has been described below.

quark-line type	dilution scheme	t_0/a	N_η	N_{ev}
fixed	(TF,SF,LI16)	4 random	6	1536
relative	(TI12,SF,LI16)	interlaced	2	1536

Table 2: Dilution scheme, source times t_0, number of noise sources N_η and number of Laplacian eigenvectors N_{ev} used to estimate quark propagation in the computation of the spectrum on Ensemble E250.

Interpolating operators: The operator basis chosen are the following:

$$\rho^+(\vec{P},t) = \frac{1}{2L^{3/2}} \sum_{\vec{x}} e^{-i\vec{P}\cdot\vec{x}} \bar{d}\Gamma u(t)\,, \tag{2}$$

where $\Gamma = \gamma_i(1 \pm \gamma_4)$ and linear combinations of $\pi\pi$ operators of the form,

$$(\pi\pi)(\vec{p}_1,\vec{p}_2,t) = \pi^+(\vec{p}_1,t)\pi^0(\vec{p}_2,t) - \pi^0(\vec{p}_1,t)\pi^+(\vec{p}_2,t)\,. \tag{3}$$

where $\vec{P}$, i.e. $\vec{p}_1 + \vec{p}_2 = \vec{P} \equiv (2\pi/L)\vec{d}$, where $\vec{d}$ is a vector of integers. We construct a correlation matrix using these interpolators for each center-of-mass momentum and its irreducible representations and employ a variational approach to extract the finite volume spectrum.

Spectrum extraction: We solve the variational problem using the Generalized EigenValue Problem (GEVP) on the correlation matrices $C(t)$ [6–8].

$$C(t)v(t,t_0) = \lambda(t,t_0)C(t_0)v(t,t_0). \tag{4}$$

where t_0 is the first time slice where the signal begins, $v(t,t_0)$ is the GEVP optimized eigenvector extracted and the eigenvalues $\lambda(t,t_0)$ represent the exponentially decaying finite-volume correlators parametrized by $A_n \exp^{-E_n(t)}$ with A_n's being the overlap factors. The finite volume energies $E_n(t)$'s are then extracted using the ratio fits [9] because it is effective in removing the contamination from higher excited states at earlier time slices.

Matrix element: We determine the matrix element of the electromagnetic current corresponding to the light quarks,

$$j_\mu^{\rm em} = \frac{2}{3}\bar{u}\gamma_\mu u - \frac{1}{3}\bar{d}\gamma_\mu d \tag{5}$$

which quantifies the overlap of the current operator at time T with the interpolating operators O defined in Eq. 2 and Eq. 3 at time T_0. This matrix element projected onto definite momentum $\vec{d}$ and irrep Λ is defined as,

$$D^{(\Lambda,\vec{d})}(T-T_0) = \left\langle j^{(\Lambda,\vec{d})}(T)\bar{O}^{(\Lambda,\vec{d})}(T_0)\right\rangle \tag{6}$$

The GEVP optimized finite volume matrix elements $\hat{D}_n^{(\Lambda,\vec{d})}(t)$ at $t = T - T_0$ are computed using the GEVP optimized eigenvectors v_n's defined in Eq. 4, as shown below:

$$\hat{D}_n^{(\Lambda,\vec{d})}(t) = (D(t), v_n)\,, \tag{7}$$

where the n represents the GEVP index. For the sake of simplicity, in the next sections we omit the $(\Lambda,\vec{d})$ notation. We construct three ratios using these overlap correlators in order to reliably extract

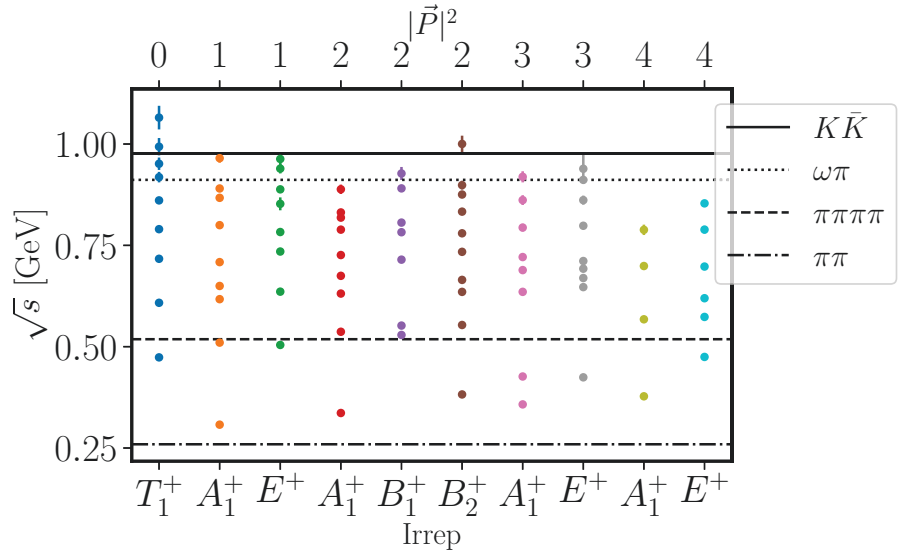

Figure 1: E250 spectrum for different irreps in different moving frames.

the desired matrix element.

$$R_1^{(n)}(t) = \left| \frac{\hat{D}_n(t)}{\sqrt{\hat{C}_n(t)\mathrm{e}^{-E_n t}}} \right|, \quad R_2^{(n)}(t) = \left| \frac{\hat{D}_n(t)}{A_n \mathrm{e}^{-E_n t}} \right|, \tag{8}$$

$$R_3^{(n)}(t) = \left| \frac{\hat{D}_n(t) A_n}{\hat{C}_n(t)} \right|$$

where $\hat{C}_n(t)$ are the GEVP optimized correlators and the A_n are the overlap factors extracted from the single exponential ratio fits to the eigenvalues extracted from GEVP. These ratios by construction are expected to plateau for asymptotically large t. It has been observed that $R_1^{(n)}(t)$ has the least noisy signal because it doesn't have contributions from the systematic uncertainties in A_n.

Vector-Vector correlator reconstruction: The vector-vector correlator in Eq (1) $G\,(x_0)$ when computed on a finite volume receives contributions from the $\pi\,\pi$ states in the $I = 1$ channel because this channel is enhanced by the existence of the $\rho(770)$ resonance. Therefore, we reconstruct the integrand using the plateau values of $R_1^{(n)}$ and the GEVP extracted energies E_n as follows:

$$G^{ud}_{n_{\max}}\,(x_0) = \frac{10}{9} \sum_{n=0}^{n_{\max}} \left| R_1^{(n)} \right|^2 e^{-E_n x_0} \tag{9}$$

Reconstruction using Time-like form factor: The VV correlator being enhanced by the ρ resonance at low energies can be reconstructed using the Time-like Pion form factor $|F_\pi(\omega)|$ as follows:

$$G^{\rho\rho}\,(x_0)_{\text{ext}} = \int_0^\infty d\omega \omega^2 \rho\left(\omega^2\right) e^{-\omega x_0} \tag{10}$$

where,

$$\rho\left(\omega^2\right) = \frac{1}{48\pi^2}\left(1 - \frac{4m_\pi^2}{\omega^2}\right)^{\frac{3}{2}} |F_\pi(\omega)|^2 \tag{11}$$

The computation of the $|F_\pi(\omega)|$ needs input from the $\rho(770)$ resonance parameters.

Extraction of resonance parameters: We employ the Lüscher quantization condition[10–12] as shown below, to compute the infinite volume resonance parameters using the finite volume energy spectrum. The Lüscher quantization condition for elastic $\pi\pi$ scattering is

$$\det\left(\mathbb{1} + \mathrm{i}t_\ell(s)(\mathbb{1} + \mathrm{i}\mathcal{M}^{\vec{P}})\right) = 0 \tag{12}$$

where $t_\ell(s)$ is parametrized by the scattering phase-shift and $\mathcal{M}^{\vec{P}}$ represents the finite volume spectrum from the frame with center of mass momentum $\vec{P}$.

3. Results and Discussion

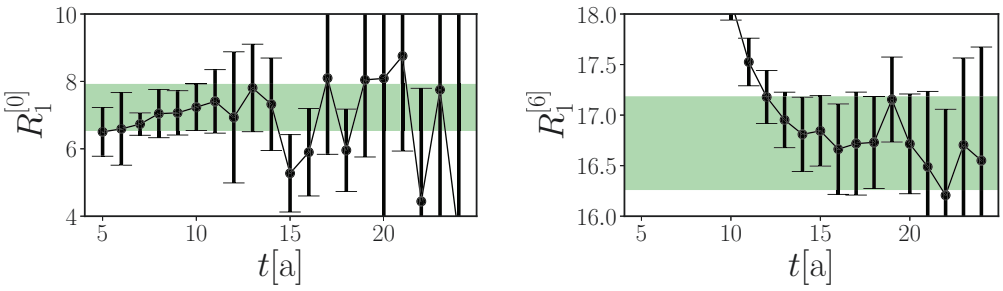

Figure 2: The matrix element between the 0^{th} energy level from GEVP and the VV correlator & 6^{th} energy level from GEVP and the VV correlator. The green band represents the selected plateau average.

The plateau average examples for two different matrix elements between two GEVP optimized scattering states and the VV correlator has been depicted in Fig. (2). The selection of the plateau is a source of systematic uncertainty in the calculation. Utilizing these $R_1^{(n)}$ plateau averages and th GEVP obtained energy levels, we reconstruct the integrand in Eq. (1). It is worth noting that the 8^{th} state reconstruction is within 1-σ interval of the 7^{th} reconstruction indicating a saturation of the n-state contributions to the VV correlator.

4. Summary

We report the status of $\pi\pi$ state reconstruction of the vector-vector correlator at the physical point pursued by the Mainz group, in order to aid the calculation of the a_μ^{hvp} contribution to $(g-2)_\mu$. The analysis is performed on an $N_f = 2+1$ CLS ensemble using the stochastic distillation framework. The calculation of the time-like pion form factor is currently underway and efforts are being made to increase the statistics.

Acknowledgments

Calculations for this project used HPC resources on the supercomputers HAWK at High-Performance Computing Center(HLRS), Stuttgart. The authors gratefully acknowledge the support of the John von Neumann Institute for Computing and Gauss Centre for Supercomputing

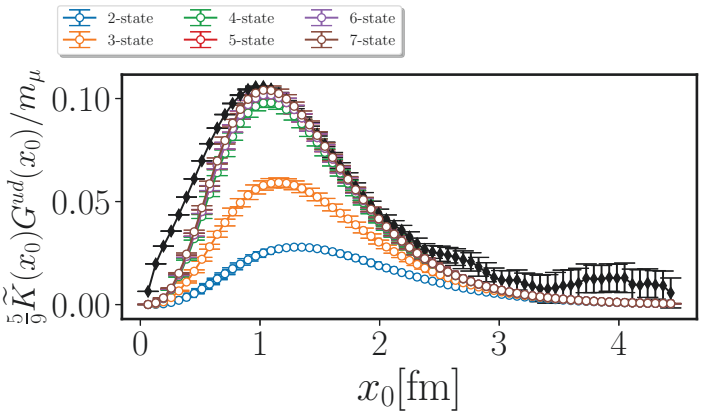

Figure 3: *n*-state reconstruction of the Integrand. The black points denote the naive computation of the VV correlator on the lattice

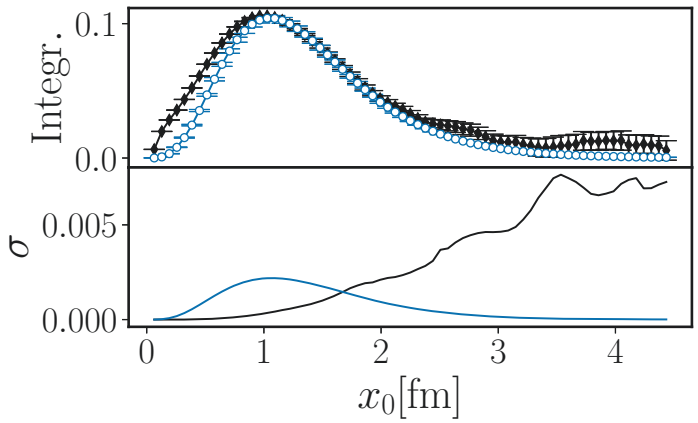

Figure 4: Exponential error reduction in the tail. This plot compares the standard deviation from the naive VV correlator computation and the 7-state reconstructed VV correlator using $\pi\,\pi$ states.

e.V.(http://www.gauss-centre.eu) for project GCS-HQCD. ADH is supported by: (i) The U.S. Department of Energy, Office of Science, Office of Nuclear Physics through the Contract No. DE-SC0012704 (S.M.); (ii) The U.S. Department of Energy, Office of Science, Office of Nuclear Physics and Office of Advanced Scientific Computing Research, within the framework of Scientific Discovery through Advance Computing (SciDAC) award Computing the Properties of Matter with Leadership Computing Resources. E250 gauge configurations were generated by DM within the CLS efforts on the supercomputers JUQUEEEN at Juelich Supercomputing Center, HAZEL HEN and HAWK at HLRS Stuttgart and MOGON II at Johannes Gutenberg University Mainz. We acknowledge computing resources provided through award 1913158 on Frontera at the Texas Advanced Computing Center (TACC). CJM acknowledges support from the U.S. NSF under award PHY-1913158. D.M. acknowledges funding by the Heisenberg Programme of the Deutsche Forschungsgemeinschaft (DFG, German Research Foundation) – project number 454605793.

References

[1] R. Gupta et al., in *39th International Symposium on Lattice Field Theory*, 1, 2023, 2301.07885.

[2] C. Alexandrou, S. Bacchio, G. Koutsou, S. Paul, M. Petschlies and F. Pittler, *PoS* **LATTICE2022** (2023) 120.

[3] D. Mohler and S. Schaefer, *Phys. Rev. D* **102** (2020) 074506 [2003.13359].

[4] Hadron Spectrum collaboration, M. Peardon, J. Bulava, J. Foley, C. Morningstar, J. Dudek, R. G. Edwards et al., , *Phys. Rev. D* **80** (2009) 054506 [0905.2160].

[5] C. Morningstar, J. Bulava, J. Foley, K. J. Juge, D. Lenkner, M. Peardon et al., *Phys. Rev.* **D83** (2011) 114505 [1104.3870].

[6] C. Michael and I. Teasdale, *Nucl. Phys. B* **215** (1983) 433.

[7] C. Michael, *Nucl. Phys. B* **259** (1985) 58.

[8] B. Blossier, M. Della Morte, G. von Hippel, T. Mendes and R. Sommer, *JHEP* **04** (2009) 094 [0902.1265].

[9] J. Bulava, B. Fahy, B. Hörz, K. J. Juge, C. Morningstar and C. H. Wong, *Nucl. Phys. B* **910** (2016) 842 [1604.05593].

[10] M. Luscher, *Commun. Math. Phys.* **104** (1986) 177.

[11] M. Luscher, *Commun. Math. Phys.* **105** (1986) 153.

[12] M. Luscher, *Nucl. Phys. B* **354** (1991) 531.